water

MDPI

Article

Factors Affecting the Morphology of Granular Sludge in Phosphorus-Accumulating Organism (PAO) and Denitrifying PAO (DPAO) Sequencing Batch Reactors

Geumhee Yun [1], Zuwhan Yun [1], Young Kim [1] and Kyungjin Han [2,*]

[1] Department of Environmental Engineering, Korea University, Sejong 30019, Republic of Korea; rmal9292@korea.ac.kr (G.Y.)
[2] Department of Environmental Engineering, Korea National University of Transportation, Chungju 27469, Republic of Korea
* Correspondence: rudwls1009@ut.ac.kr; Tel.: +82-43-841-5356

Abstract: This study aimed to investigate the influencing factors and characteristics of granule morphology through approximately 500 d of long-term monitoring of two types of anaerobic–aerobic phosphorus-accumulating organism (PAO) and anaerobic–anoxic denitrifying PAO (DPAO) sequencing batch reactors (SBRs). The results show that granules were present in the DPAO SBR and PAO SBR after 200 d and 250 d of operation, respectively. The average diameters of the granules were 2.2 ± 0.7 mm in the DPAO SBR and 0.4 ± 0.3 mm in the PAO SBR, respectively. The DPAO granular sludge contained rod-shaped microorganisms, whereas the PAO granular sludge contained cocci-type microorganisms. A precipitated core consisting of hydroxyapatite was found in the DPAO granules. A comparative analysis conducted under various operating conditions revealed that the availability and type of the electron acceptors (EAs) may have a significant impact on granulation. This observation suggests that the presence and diversity of EAs are crucial factors for the development of different granule sizes and morphologies.

Keywords: wastewater treatment plant; granular sludge morphology; phosphorus-accumulating organism; sequencing batch reactor

Citation: Yun, G.; Yun, Z.; Kim, Y.; Han, K. Factors Affecting the Morphology of Granular Sludge in Phosphorus-Accumulating Organism (PAO) and Denitrifying PAO (DPAO) Sequencing Batch Reactors. *Water* **2023**, *15*, 4108. https://doi.org/10.3390/w15234108

Academic Editors: Mehrab Mehrvar, Edgar Quiñones-Bolaños, Ciro Bustillo-Lecompte and Samira Ghafoori

Received: 18 October 2023
Revised: 21 November 2023
Accepted: 25 November 2023
Published: 27 November 2023

1. Introduction

Phosphorus and nitrogen are limiting macronutrients in aquatic ecosystems. Therefore, for effective surface water quality management, it is essential to remove these nutrients in the wastewater treatment plant (WWTP). Recently, there has been no change in Korea's effluent water quality standard for the nitrogen content. The permitted phosphorus content has become more stringent since 2012, with a decreased limit of 0.2–0.5 mg/L from 2.0 mg/L [1], depending on the water bodies, and there is scope for further reductions in the permissible nitrogen and phosphorus contents. Therefore, effective nutrient removal in WWTPs is essential for water quality management and compliance with Korean regulatory standards.

The enhanced biological phosphorus removal (EBPR) process can effectively manage phosphorus, which is a critical nutrient for eutrophication. EBPR of phosphorus-accumulating organisms (PAO) under alternating anaerobic–aerobic (An–Ox) conditions facilitates biological phosphorus removal. Biological nutrient removal (BNR) of denitrifying PAO (DPAO) can simultaneously remove P and N because DPAO utilizes NO_3^--N as an electron acceptor (EA) and does not use organic substances in the anoxic zone [2]. Thus, DPAO in an An–Ax SBR would be an excellent alternative to simultaneously remove N and P in a WWTP.

Conventional activated sludge (CAS) systems have been widely used in WWTPs over the past century to protect the water environment. However, CAS faces challenges in

meeting increasingly stringent water quality standards, primarily owing to operational issues such as sludge bulking. The self-aggregated granular sludge system is a novel technology employed for biological wastewater treatment. Compared with CAS, the granular system offers several advantages, including improved sludge settleability and the capacity to accommodate high organic loading. Therefore, the granulation system has undergone extensive investigation in both laboratory-scale reactors and a few WWTPs in recent years [3–11]. Recent studies have shown that granular sludge can form in PAO and DPAO sequencing batch reactors (SBRs) [12,13]. This is an important finding because various types of microbes, such as nitrifiers, denitrifiers, PAOs, and DPAOs, reside within aerobic granules, forming the basis for biological nitrogen and phosphorus removal [14]. Therefore, the aerobic granular process enables the simultaneous achievement of organic carbon, nitrogen, and phosphorus removal through the process of simultaneous nitrification, denitrification, and phosphorus removal (SNDPR) [15]. Moreover, as some PAOs can accumulate polyphosphate under anoxic conditions, the presence of DPAOs [16] in the granules can enhance the phosphorus removal efficiency while minimizing oxygen utilization [15,16].

Because DPAOs use nitrate under anoxic conditions, they can decrease the amount of oxygen required to oxidize poly-β-hydroxy-alkanoates (PHAs) in the aerobic zone and reduce the utilization of the chemical oxygen demand (COD) [17,18]. Using DPAOs for carbon source conservation is essential because there is a shortage of carbon sources for BNR in sewage in Korea. Although phosphorus can be removed by treating it with chemicals, there is no alternative for removing nitrogen other than employing biological treatment methods; therefore, efficient utilization of the carbon source in sewage is considered to be a critical concern for the future, particularly as effluent water quality standards continue to become more stringent. Therefore, DPAO granular sludge has the potential to efficiently address the increasingly stringent effluent water quality standards and eutrophication issues and to operate an efficient WWTP that maximizes the utilization of the carbon sources in influent water.

Angela et al. [13] found that under An–Ox SBR operating conditions, inorganic materials crystallized into hydroxyapatite (HAP) within the interior of granular sludge. However, in our previous study [18], crystalline structures were observed in the interior of granular sludge only in a DPAO SBR. Recently, the formation of HAP granular composites to improve the settleability of sludge has been reported as a potentially cost-effective approach for the removal of nitrogen and phosphorus in wastewater treatment. Before using these granules for applications, research is needed into the factors that lead to the formation of hydroxyapatite (HAP) in the granules [19–22]. Various additional factors also influence sludge granulation, including the height-to-diameter (H/D) ratio of the reactor [23], volume exchange ratio in the SBR [7], organic loading rate [10], hydraulic shear force, sludge settling time [24,25], and starvation time [26]. In anaerobic and aerobic granulation, extracellular polymeric substances (EPSs) play a critical role [27]. However, the formation mechanism of granular sludge has not been sufficiently investigated, and the theories concerning granule formation are still unclear. Consequently, the characterization of precipitates inside aerobic granules is still a relatively unexplored field.

Therefore, in this study, we attempted to investigate the factors affecting granule formation in a DPAO SBR and a PAO SBR through long-term monitoring for approximately 500 d and the analysis of various published literature data. Specifically, the morphological characteristics of granular sludge during the long-term operation were investigated using an environmental scanning electron microscope (ESEM), the sludge volume index (SVI), the size distribution, EPSs, and X-ray diffraction (XRD). Potential influencing factors were investigated through comparative analysis under various operating conditions using reference data from approximately 250 studies on granulation.

2. Materials and Methods

2.1. Reactor Configuration and Operational Conditions

This study experimentally investigated the characteristics of granular sludge to differentiate between An–Ox (PAO) and An–Ax (DPAO) by operating two identical lab-scale SBRs. Each lab-scale SBR (Figure S1) comprised a cylindrical acrylic reactor with a maximum volume of 5.9 L. The SBR had an aspect ratio of 1.9 (diameter 170 mm, height 320 mm) at a total workload of 2.5 L. The decant/feed volume was 60% of the total volume for each cycle. The reactor was operated with a predefined process using a programmable logic controller (PLC) at room temperature. A mechanical stirrer was used for mixing (35 ± 10 rpm) within the reactor during operation (approximately 35% of the volume).

Activated sludge obtained from the Seoul Joongrang Municipal WWTP was used as the seed sludge. The influent of both reactors was supplied thrice a day at 8 h intervals at a rate of 3.4 L/cycle. The operation cycle for the An–Ax SBR for DPAO growth was set as follows: fill (0.5 h), anaerobic (2.5 h), anoxic (4 h), settling (0.5 h), and decant (0.5 h). The operation cycle for the An–Ox SBR for PAO growth was set as follows: fill (0.5 h), anaerobic (2.5 h), aerobic (4 h), settling (0.5 h), and decant (0.5 h) (Figure S2). In the An–Ax SBR, an external EA was added at 15 mg NO_3-N/L to the initial anoxic period. For the aerobic condition in the An–Ox SBR operation, an oval air stone with a diameter of 140 mm and an air pump (LP-40A, Yong-nam Co, Busan, Republic of Korea) were installed for aeration such that the flow rate was 20 L/min and the gas flow rate was 1.5 m/s. Subsequently, aeration was supplied to maintain an oxic DO concentration of approximately $2-3$ mg/L, and the solid retention time (SRT) was maintained for 20 d during the steady-state operation based on the measured total suspended solids (TSS) and effluent TSS concentrations in both SBRs. The SRTs of the An–Ax SBR and An–Ox SBR were approximately 27 and 25 d, respectively. The MLSS of the An–Ax SBR was 2226 mg/L, whereas that of the An–Ox SBR was 2812 mg/L on average.

2.2. Synthetic Wastewater

Synthetic wastewater was prepared using propionic acid (HPr) as the carbon source, NH_4Cl and KNO_3 as the nitrogen sources, and KH_2PO_4 as the phosphate source. The reason for using HPr was to exclude glycogen-accumulating organisms (GAOs), which are known to inhibit EBPR and selectively cultivate PAO and DPAO [28,29]. Subsequently, a known trace metal concentration (0.1 mg/L) was added [18,30]. Various forms of nitrogen were used as nitrogen sources. For the N in the An–Ax SBR, 10 mg/L of NH_4^+-N was injected into the influent for microbial synthesis. In the An–Ox SBR, 25 mg/L of NH_4^+-N was injected into the influent so that the TN concentration of the An–Ax SBR would be equal to that of the An–Ox SBR. KH_2PO_4 supplied phosphorus. For $NO_3^- - N$, the KNO_3 reagent was added at a concentration of 15 mg/L so that the DPAO could be used as an EA in the anoxic condition. For comparing the test results using selective culture with DPAO and PAO, both the An–Ax SBR and An–Ox SBR were supplied with the same influent C/N/P ratio (25/3.5/1), organic loading rate (OLR) (0.26 $kg/m^3 \cdot d$), and pH range (5–6). The detailed synthetic wastewater composition is provided in Table S1.

2.3. Data Analysis

The granular sludge characteristics were examined using an optical microscope, ESEM, XRD, SVI, size distribution, EPS, and soluble microbial product (SMP). To determine the potential factors causing granulation, we selected 34 studies that determined the sizes of granules out of approximately 250 studies on granulation. We correlated the granule sizes with various operating parameters in the reference data. The operating conditions included the OLR, SVI, MLSS, SRT, hydraulic retention time (HRT), H/D ratio, setting time in the SBR cycle, aeration intensity, food-to-microorganism ratio (F/M) ratio, and EPS. The Statistical Package for the Social Sciences (SPSS) for Windows, Version 21.0. program (IBM Corporation, Armonk, NY, USA) was used to compare the Pearson correlations between the granule size and various operating parameters. Pearson correlation evaluates whether

statistical evidence exists for a linear relationship among the same pairs of variables in the population. This is represented by the population correlation coefficient, ρ ("rho"). The PHREEQC Version 3 software (Minteq.v3.1 database) was used to calculate the chemical equilibrium for the concentration of components (NO_3^-, PO_4^{3-}, and Ca^{2+}) in the DPAO SBR at the end of the anaerobic condition.

2.4. Analytical Methods

The complex gel-like matrix of biomacromolecules containing nucleic acids, lipids, polysaccharides, proteins, and humic substances located on or just outside the bacterial cells in cohesive and granular sludge is formed of EPSs. It plays an important role in microbial adhesion and aggregation. Therefore, the EPS concentrations of both SBRs were measured. In this study, the EPS concentration was measured following the Frϕlund [31] method, which utilized the cation exchange resin, which might reduce the chemical contamination. The carbohydrate content of the EPSs was measured using the phenol–sulfuric acid method, and the protein content was measured using the Lowry [32] method. An optical microscope (JSB-133, Green sci., Seoul, Republic of Korea) was used to observe the morphology of the granules. The granule core was analyzed via XRD (TTK-450 model, Anton Paar, Austria). The granule size and distribution were analyzed using the sieve test. Once the TSS from each sieve was determined, the percentage of the total weight was calculated for each granule class size (0.15, 0.212, 0.425, 0.6, 0.85, 1.0, 1.7, and 2.0 mm). The morphological characteristics of the anoxic and aerobic sludge obtained from the PAO and DPAO reactors were examined using an optical microscope (JSB-133, Green sci., Seoul, Republic of Korea) and ESEM (FEI XL-30 FEG, Philips, Amsterdam, The Netherlands). Each was harvested via centrifugation (10,000× *g*) for 10 min. For accurate ESEM measurements, the samples were fixed to the sample holder with silver paste. The granule cores were analyzed via XRD (TTK-450 model).

The dissolved oxygen (DO) was measured using a YSI (YSI Incorporated, Yellow Springs, OH, USA) ProPlus multiparameter equipped with a quaternary cable flow cell. The instrument was calibrated weekly.

3. Results and Discussion

3.1. Morphological Characteristics of Granules

In our previous study, EBPR was successfully performed in PAO and DPAO SBR systems [18]. Granules were observed in the PAO and DPAO SBRs after 200 d of operation (Figure 1). The average diameter of the DPAO granules was 2.2 ± 1.7 mm, which was approximately five times larger than that of PAO SBR granules (0.4 ± 0.3 mm). A crystallized core was found in the interior of the granular sludge only in the DPAO SBR (Figure 1a).

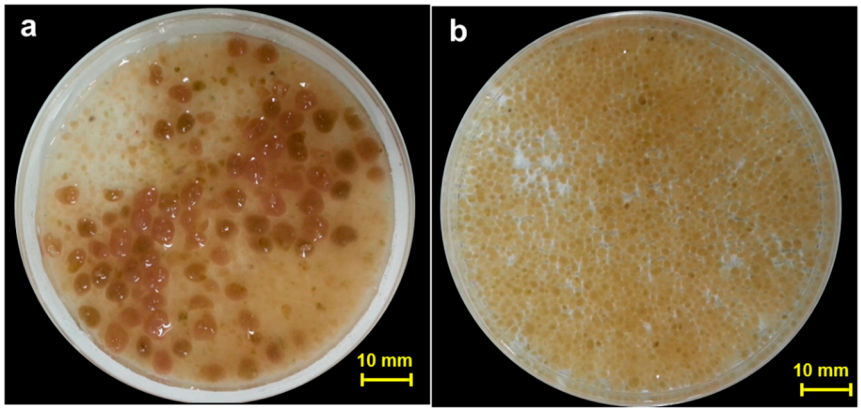

Figure 1. Images of granules in (**a**) the DPAO SBR and (**b**) the PAO SBR after 200 d of operation.

The images of granules in the DPAO SBR on the 370th day of operation are shown in Figure 2. Optical images (×40) acquired on the 180 d showed a fuzzy core within

the granules. The core became visible after 250 d. On the 370 d of operation, a white precipitate was observed in the core of the granules. In contrast, no core was observed in the An–Ox granules.

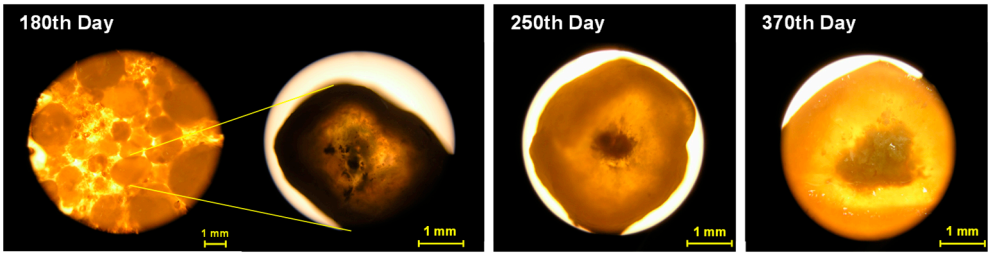

Figure 2. Optical images of DPAO granules after 370 d of operation.

XRD analysis (not shown here) confirmed that the core material was very similar to hydroxyapatite (HAP; $Ca_5(PO_4)_3(OH)$). Angela et al. [13] reported inorganic materials crystallized in a hydroxyapatite form in the interior of granular sludge, suggesting that the core precipitation resulted from a chemical reaction. Our PAO granules did not contain such a core precipitate. Although the operating conditions were same for both the studies, the granule size, density, crystal, and shape were considerably different.

The results of the XRD analysis [18] showed that the peaks of the sediment in the granule core and the HAP spectrum matched, confirming that the core material was very similar to HAP. Inorganic precipitates in PAO granules have not been observed so far. Among other recent studies that studied sludge granulation in anaerobic–oxic SBRs [12,13,33], Angela et al. [13] reported hydroxyapatite (HAP)-like crystals in the core of the granules with a 2 mm diameter. We also observed HAP in the core of the granules with a 2.5 mm diameter in the DPAO SBR (Figure 2), but not in the PAO SBR. Notably, biologically induced phosphate precipitation has been reported in activated sludge systems [34]. Calcium phosphate precipitates form due to P release under anaerobic conditions and a pH of 7.0–8.5 [35,36]. Most aerobic granular sludge reactors were operated in the pH range of 6–8, and the negative effects of the pH were reported only at very high or low values. Tests performed on aerobic granules, related granules, and EPS extracts [37,38] suggest that granule disintegration through dissolution of the dominant structural exopolysaccharide will occur above pH 8. Likewise, alginate-like EPSs are stable over a wide range of pH values in the presence of appropriate divalent cations, especially Ca^{2+}, which can be used to crosslink the building blocks of alginic acid polymers [39]. In the DPAO SBR experiment, the pH first decreased from 8.5 to 8.0 under anaerobic conditions and then increased to 8.85 under anoxic conditions. However, for the PAO SBR, the average pH at the end of the anaerobic and aerobic conditions was 6.89 and 7.1, respectively. Therefore, no sediment was found. The pH difference between the DPAO and PAO SBRs is due to the different biological responses of each system.

3.2. Effect of PH on HAP Precipitation

The saturation index (SI) calculation for different minerals for the supernatant, established for each pH, is shown in Figure 3. The SI was calculated using the Minteq.v4 database (PHREEQC Version 3, software), with the pH and concentrations (NO_3^-, PO_4^{3-}, Ca^{2+}) measured in the bulk. With respect to calcium phosphates, the SIs for Am1, Am2, Beta, OCP, and HAP were higher than 0 at a higher pH, i.e., these minerals were considerably oversaturated. The SI for amorphous calcium phosphate varied from 4.92 to <0.39 at a pH range of 7–10. Finally, the highest value of the SI (6.79–16.29) at pH 7–10 was obtained for hydroxyapatite, i.e., the most stable phase among the calcium phosphates showed oversaturation conditions throughout the experiment. This suggests that HAP was found to be able to be formed at pH 7 or higher.

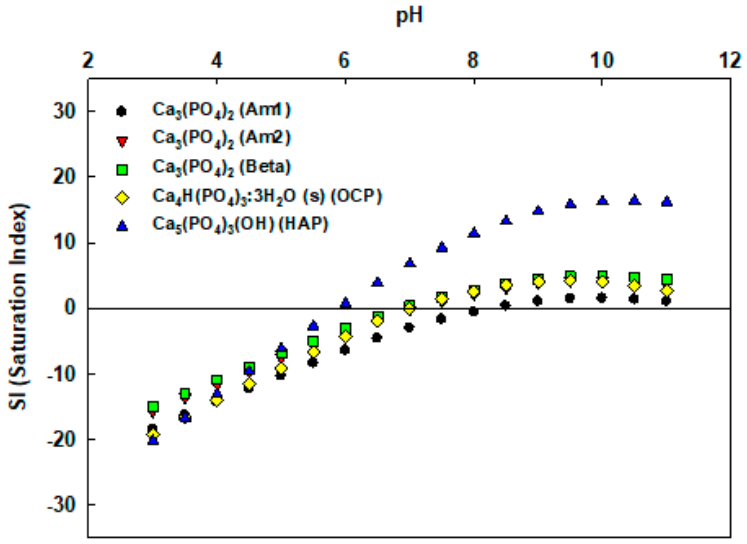

Figure 3. Saturation index calculations for different minerals in the supernatant were performed for each pH (Minteq. ver. 3.1).

A precipitated core primarily comprising hydroxyapatite ($Ca_5(PO_4)_3(OH)$) was found in the DPAO granules. The pH during the anoxic period of the DPAO SBR was maintained at 8.85 ± 0.5 because of the denitrification and P uptake. The higher pH provided the necessary conditions for HAP formation in the DPAO granules. Core precipitation was not observed within the PAO granules. The pH of the An–Ox SBR was maintained between 6.89 and 7.1. According to the literature [40,41], the pH difference between the two systems suggests that they have contributed to the formation of core precipitation. The different biological reactions in each system caused the pH difference between the DPAO and PAO SBRs. Moreover, bioreactions such as nitrification, denitrification, and EBPR led to the pH gradients responsible for precipitation in the activated sludge. This suggests that the pH influence was more substantial for HAP formation in the DPAO granules than in the PAO granules.

3.3. Possible Factors Influencing Granule Formation

From a physicochemical perspective, the EPSs covering the cell surface can be regarded as polyelectrolytes adsorbed on colloidal particles, which can change the physicochemical properties of the cell surface, such as the charge, hydrophobicity, and other properties. Since the surface properties of bacteria are essential for flocculation, attachment, and granulation, EPSs can play an important role in the flocculation and granulation of activated sludge [27]. The EPS and SMP contents per VSS in the SBRs are shown in Figure 4. The EPS content per unit biomass in the DPAO granular sludge with a bigger particle diameter (36.07 mg EPS/g VSS) was 53% more than in the PAO granular sludge (23.93 mg EPS/g VSS) (Figure 4a). The SMP contents per unit of biomass were 1.78 and 2.92 mg SMP/g VSS, respectively (Figure 4b). Additionally, the PN concentrations in the EPSs were 2.3-fold (An–Ox SBR) and 3.5-fold (An–Ax SBR) higher than the PS concentrations in both SBRs (Figure 4). Jorand et al. [42] suggested that PS is primarily hydrophilic. PN is primarily hydrophobic, indicating that the proteinous EPSs may play a significant role in sludge granulation.

To determine the possible factors causing significant differences in the granule formation, we compared various operating conditions of both SBRs. The results are listed in Table 1.

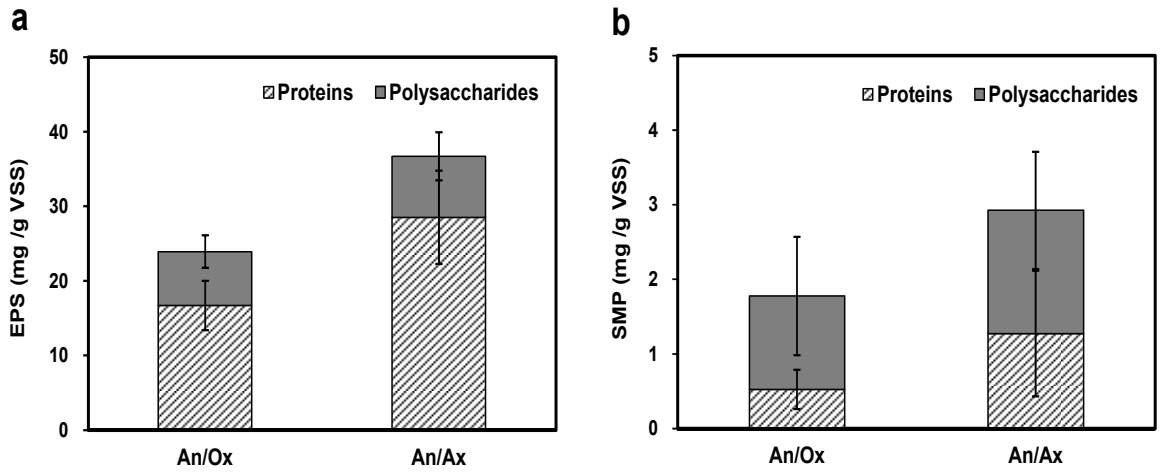

Figure 4. EPS concentrations in the EPSs (**a**) and SMP (**b**) in both SBRs.

Table 1. Comparison of the operating conditions for both SBRs.

	Factors	An–Ox SBR (PAO)	An–Ax SBR (DPAO)	Difference
Reactor operating condition	OLR (kg/m^3·d)	0.49	0.49	
	Aver. SRT (day)	34.56	40.02	×
	HRT (h)	13.9	13.9	
	Reactor vol. (L)	5.9	5.9	
	H/D ratio	1.9	1.9	
	Settling time (min)	30	30	
	C/N ratio	8.3	8.3	
	F/M ratio	0.12	0.12	
	MLSS (mg/L)	2812	2226	
	Aeration intensity (cm/s)	1.46	-	
	Aver. pH An	7.28	7.34	×
	Aver. pH Ox	6.78	-	×
	Aver. pH Ax	-	8.85	×
	DO (mg/L)	3	0.04	×
	Type of electron acceptor	Molecular O_2	Bounded O_2 (NO_3)	×
Granule characteristics	Core	No	Yes	×
	Aver. diameter (mm)	0.41	2.20	×
	SVI_{30} (mL/g)	84	97	
	Aver. EPS conc. (mg/g vss)	23.93	36.07	×

The significant differences in the operating conditions were related to the SRT, pH, DO, and type of EA. The EPS content in the granules was another crucial difference. Figures 5 and 6 show plots of the values observed in this study (closed circles) and the reference granule sizes (numbered open circles) versus the operating conditions as extracted from the references (all data used in Figures 5 and 6 are presented in Table 2). Table 2 shows the Pearson correlations (p) between the granule size and various operating parameters.

As shown in Figure 5a, the reactor H/D ratio and granule size were unrelated ($p = -0.292$). The aeration intensity is an important parameter for aerobic granulation [4,21,36]. In particular, Kong et al. [23] claimed that linear velocity should be maintained at >2.5 cm/s for stable granulation. The results presented in Figure 5b indicate that a lower aeration intensity can induce granule formation, albeit of various sizes. This indicates a weak relationship ($p = -0.250$) between the aeration intensity and granule size. Adav et al. [8] reported that a higher OLR was preferred for granulation. However, in our study, granules were formed at various ranges of the OLR (Figure 5c). Moreover, various sizes of granules were formed at a lower F/M value of 0.2 kg COD/kg MLSS·d (Figure 5d). The granule formation at the reactor HRT lasted from 1 h to 24.5 h (Figure 5e), while the SRT varied from 3 to 46 d (Figure 5f). The mean SRT of the

DPAO SBR was approximately 40.02 d, which was slightly longer than that of the PAO SBR (34.56 d). It is challenging to correlate the granule size and SRT and HRT. Similarly, Li et al. [43] concluded that no significant relation could be established between the SRT and granule size.

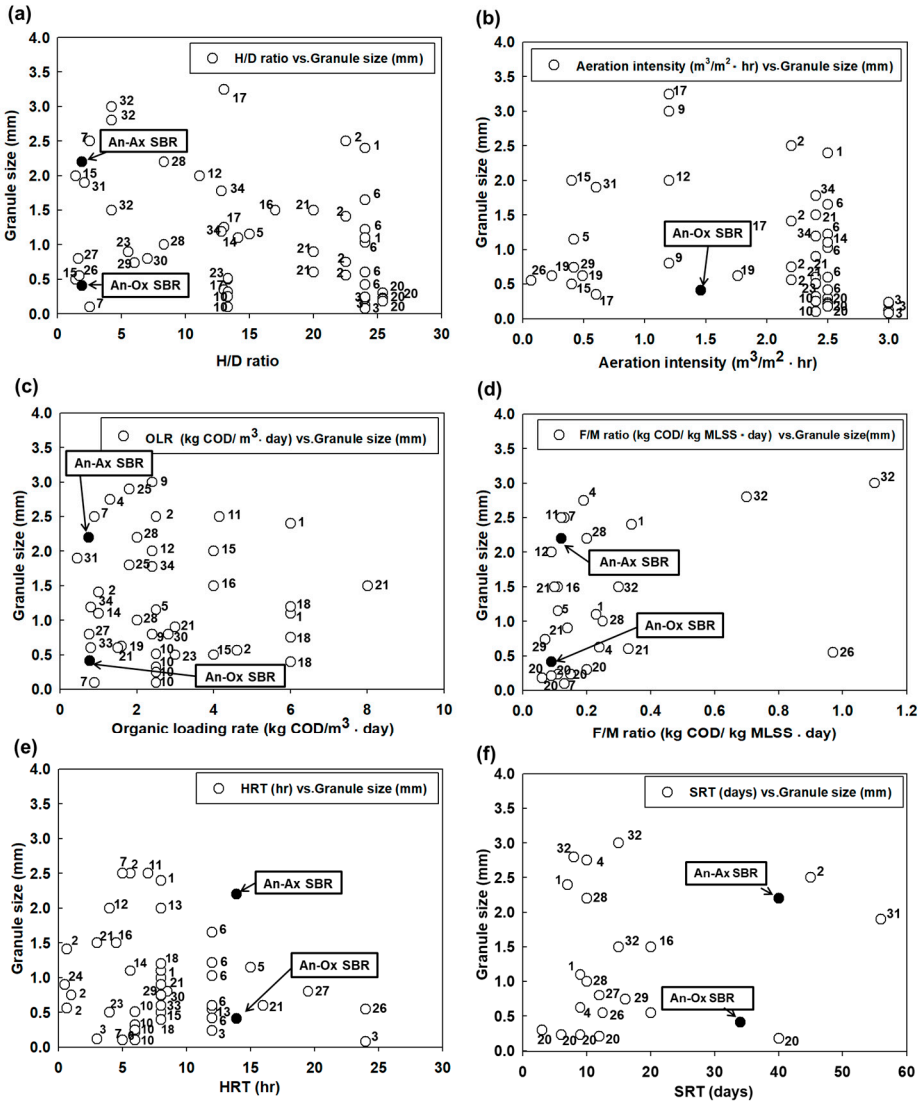

Figure 5. The relationship between the granule size and H/D ratio (**a**), Aeration intensity (**b**), OLR (**c**), F/M ratio (**d**), HRT (**e**) and SRT (**f**) obtained from 34 references was compared with our results.

The settling times from most of the reference data (Figure 6a) were <10 min for the SBR operating cycle. There was no significant relationship between the settling time during the SBR operating cycle and the granule size ($p = -0.203$). In addition, the granule size was not related to the SVI ($p = 0.047$), which indicates granule settleability, as shown in Figure 6b. The comparison suggests that physical characteristics, such as the granule density, may govern the SVI and size. In the granulation studies, the operating MLSS varied from 2000 to 10,000 mg/L (Figure 6c). The granule size did not increase with an increasing MLSS concentration ($p = 0.172$). This finding contrasts with those of Muda et al. [44], who reported that a higher biomass accumulation in the reactor may be a prerequisite for granulation. EPSs act as a binding agent in biological systems, including aerobic-activated sludge processes and anaerobic granular systems such as UASB. The question concerning the utility of EPS data is that it comprise the results of complex biological process rather than an operating tool to control the granulation. The excessive variation in EPS measurement methods is another challenge when conducting accurate comparisons. Thus, oversimplified measurement of the protein and carbohydrate contents in granules

may not provide reliable comparison results, as noted for other water quality parameters in the Standard Methods (2005). Although various references are available, however, the relation between the EPSs and granule size has not been studied extensively. As the rationale for EPS extraction and analysis varies widely, the results cannot be compared reliably. Granulation can be achieved at a low EPS concentration, indicating that a higher EPS concentration is not a prerequisite for granule formation (Figure 6d). However, the measurement of the protein and carbohydrate contents in granules suggested that the more prominent granules produced in the DPAO SBR contained more proteins than the smaller granules produced in the PAO SBR. However, Jorand et al. [42] reported that the protein content of the EPSs in activated sludge generally exhibited hydrophobicity, the role of hydrophobic protein in forming larger granules.

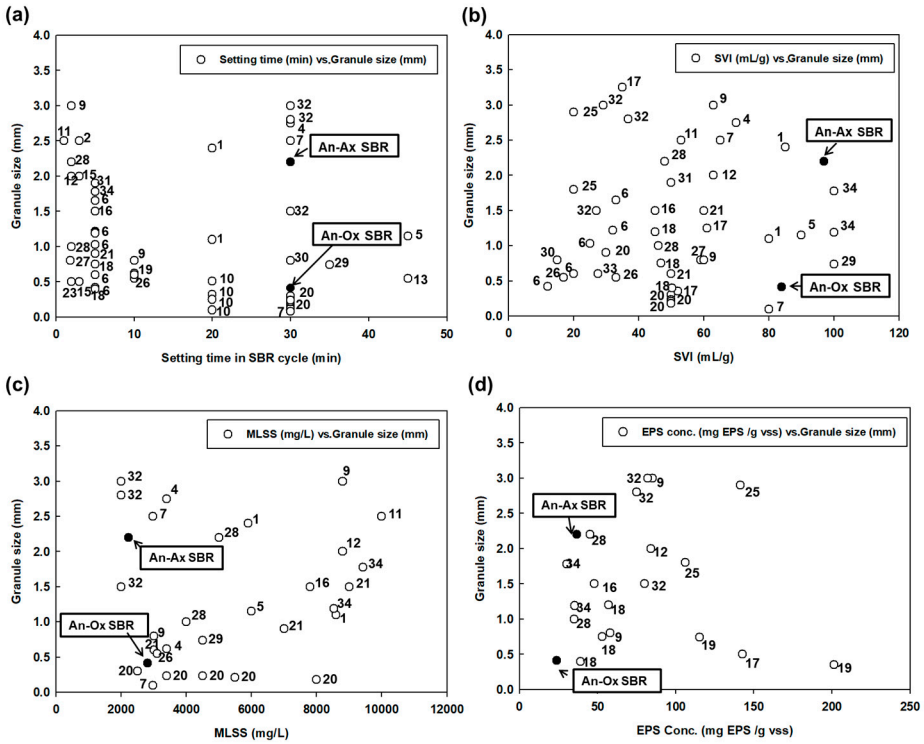

Figure 6. The relationship between the granule size and settling time (**a**), SVI (**b**), MLSS (**c**) and EPS concentration (**d**) obtained from 34 references was compared with our results.

Table 2. Pearson correlations between the granule size and various operating parameters.

Operating Parameters	Variable Number (n)	Pearson Correlation (p)
H/D ratio	56	−0.292 *
OLR ($kg/m^3 \cdot d$)	42	−037
SVI (mL/g)	48	0.047
MLSS (mg/L)	32	0.172
SRT (d)	24	0.160
HRT (h)	46	−0.160
Settling time (min)	58	−0.203
Aeration intensity (cm/s)	47	−250
F/M ratio	28	0.208
Avg. EPS conc. (mg/g vss)	21	−0.012

Note: * $p < 0.05$.

3.4. Granulation and EA

The type of EA (O_2 or NO_3^- in this study) is another key factor that affects the granulation process and morphology. The nitrate solution was used as the sole EA in the DPAO SBR and was added at the beginning of the anoxic condition. The nitrate, injected

during the initial 15 min of the anoxic period, was rapidly consumed during denitrification of the denitrifying PAO in the DPAO SBR. The granulation environment in the DPAO SBR more closely resembled that in a UASB, where the firm and dense cores are loosely covered with an anaerobic biofilm. Based on these results, we propose that both the availability and types of the EA are crucial for granulation. Figure 7 depicts the relationship between EAs and various biological granulation processes. The granules developed in this study (for both the DPAO SBR and PAO SBR) are depicted as circles. In contrast, the bars represent the range of granule sizes extracted from the 34 reference data sources.

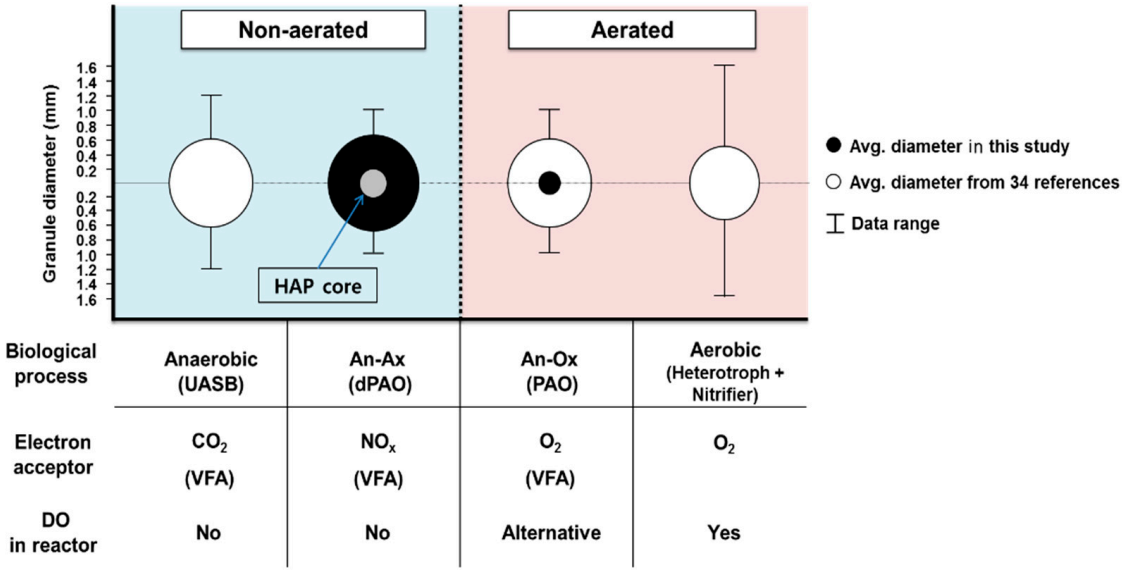

Figure 7. Comparison of various characteristics of biological granules. Bars represent the range of the granule size, while open circles denote the averaged granule diameters extracted from 34 references (34 references are listed in Table S2).

UASB granules, produced without free oxygen, have a firm, elongated structure with a dense core [45,46]. The DPAO granules from this study exhibited a relatively complex and inert core with a dense structure. However, aerobic granules typically have a loose, soft, and relatively irregular structure [47–49]. The An–Ox granules showed small and relatively dispersed growth because of the environmental stresses caused by the alternating supply of the EA. Therefore, the type of the EA is considered to play an essential role in determining the morphological characteristics.

4. Conclusions

The purpose of this study was to determine the possible factors affecting the morphology of sludge granules. This study analyzed granules from the alternating conditions of a DPAO SBR and a PAO SBR. In both reactors, unstable EBPR was observed at the initial stage of operation, but after approximately three months, stable EBPR was demonstrated successfully. Sludge granulation was observed after 200 d and 250 d of PAO SBR and DPAO SBR operation, respectively. The possible factors were investigated through a comparative analysis under various operating conditions using reference data from approximately 250 studies on granulation. In addition, we identified the granule formation mechanism based on the primary research results. The average diameter of the DPAO granules was 2.2 ± 1.7 mm, approximately five times larger than that of the PAO granules. The DPAO SBR developed granules with a dense hydroxyapatite core. Various conventional parameters, including the EPSs, yielded no clear correlation. These findings suggest that the availability and type of the EA (O_2 and NO_3^- in this study) are crucial influencing factors for different granule sizes and morphologies. The formation of the HAP core in the DPAO granules can be explained by the alkaline conditions, which aid HAP precipitation. These

findings are expected to shed light on the relatively unexplored field of granule formation mechanisms, contributing to optimizing wastewater treatment and compliance with regulatory standards in Korea. Further studies are needed to expand the range of applications of granular sludge and to increase the ability to predict the behavior and performance of granular sludge processes.

Supplementary Materials: The following supporting information can be downloaded at: https://www.mdpi.com/article/10.3390/w15234108/s1, Figure S1: Diagram(left) and image(right) of lab-scale SBRs; Figure S2: Schematic of lab-scale SBRs operational condition for biological nutrient removal in (a) the An-Ax SBR and (b) the An-Ox SBR; Table S1: Composition of synthetic wastewater; Table S2: Summary of 34 references and operating results of this study.

Author Contributions: G.Y.: Conceptualization, writing—original draft preparation, formal analysis; Z.Y.: Investigation, writing—review and editing; Y.K.: Investigation, writing—review and editing; K.H.: Investigation, writing—review and editing, supervision. All authors have read and agreed to the published version of the manuscript.

Funding: This research was supported by the Korea Ministry of Environment and the Technology Institute (KEITI) as the Subsurface Environmental Management (SEM) project (2018002480005 and 2021002470002). This research was also supported by the Korea Environment Industry and Technology Institute (KEITI) through the project to develop eco-friendly new materials and processing technology derived from wildlife, as funded by Korea Ministry of Environment (2021003270007). This research was also supported by the National Research Foundation of Korea through the basic science research program, as funded by the Korea Ministry of Science and ICT (2022R1F1A1068350).

Data Availability Statement: Data are contained within the article and Supplementary Materials.

Conflicts of Interest: The funders had no role in the design of the study; in the collection, analyses, or interpretation of data; in the writing of the manuscript; or in the decision to publish the results.

References

1. Ministry of the Environment (MOE) in Korea. Enforcement Regulations of Sewerage and Drainage Law. Available online: https://elaw.klri.re.kr/eng_mobile/newLawViewer.do?hseq=62188&type=tot&key=%ED%95%98%EC%88%98%EB%8F%84%EB%B2%95%20%EC%8B%9C%ED%96%89%EB%A0%B9&pCode=&pName= (accessed on 22 October 2023).
2. Kerrn-Jespersen, J.P.; Henze, M. Biological phosphorus uptake under anoxic and aerobic conditions. *Water Res.* **1993**, *27*, 617–624. [CrossRef]
3. Morgenroth, E.; Sherden, T.; van Loosdrecht, M.C.M.; Heijnen, J.J.; Wilderer, P.A. Aerobic granular sludge in a sequencing batch reactor. *Water Res.* **1997**, *31*, 3191–3194. [CrossRef]
4. Beun, J.J.; Hendriks, A.; van Loosdrecht, M.C.M.; Morgenroth, E.; Wilderer, P.A.; Heijnen, J.J. Aerobic granulation in a sequencing batch reactor. *Water Res.* **1999**, *33*, 2283–2290. [CrossRef]
5. Tay, J.H.; Liu, Q.S.; Liu, Y. Microscopic observation of aerobic granulation in sequential aerobic sludge blanket reactor. *J. Appl. Microbiol.* **2001**, *91*, 168–175. [CrossRef] [PubMed]
6. Yang, S.F.; Tay, J.H.; Liu, Y. Inhibition of free ammonia to the formation of aerobic granules. *Biochem. Eng. J.* **2004**, *17*, 41–48. [CrossRef]
7. Liu, Y.; Tay, J.H. State of the art of biogranulation technology for wastewater treatment. *Biotechnol. Adv.* **2004**, *22*, 533–563. [CrossRef]
8. Adav, S.S.; Lee, D.J.; Lai, J.Y. Effects of aeration intensity on formation of phenol-fed aerobic granules and extracellular polymeric substances. *Appl. Microbiol. Biotechnol.* **2007**, *77*, 175–182. [CrossRef]
9. Coma, M.; Puig, S.; Balaguer, M.D.; Colprim, J. The role of nitrate and nitrite in a granular sludge process treating low-strength wastewater. *Chem. Eng. J.* **2010**, *164*, 208–213. [CrossRef]
10. Lochmatter, S.; Maillard, J.; Holliger, C. Nitrogen removal over nitrite by aeration control in aerobic granular sludge sequencing batch reactors. *Int. J. Environ. Res. Public Health* **2014**, *11*, 6955–6978. [CrossRef]
11. Zhang, H.; Dong, F.; Jiang, T.; Wei, Y.; Wang, T.; Yang, F. Aerobic granulation with low strength wastewater at low aeration rate in A/O/A SBR reactor. *Enzym. Microb. Technol.* **2011**, *49*, 215–222. [CrossRef]
12. Wu, C.Y.; Peng, Y.Z.; Wang, S.Y.; Ma, Y. Enhanced biological phosphorus removal by granular sludge: From macro- to micro-scale. *Water Res.* **2010**, *44*, 807–814. [CrossRef] [PubMed]
13. Angela, M.; Béatrice, B.; Mathieu, S. Biologically induced phosphorus precipitation in aerobic granular sludge process. *Water Res.* **2011**, *45*, 3776–3786. [PubMed]

14. He, Q.; Zhang, W.; Zhang, S.; Wang, H. Enhanced nitrogen removal in an aerobic granular sequencing batch reactor performing simultaneous nitrification, endogenous denitrification and phosphorus removal with low superficial gas velocity. *Chem. Eng. J.* **2017**, *326*, 1223–1231. [CrossRef]
15. Yilmaz, G.; Lemaire, R.; Keller, J.; Yuan, Z.G. Simultaneous nitrification, denitrification, and phosphorus removal from nutrient-rich industrial wastewater using granular sludge. *Biotechnol. Bioeng.* **2008**, *100*, 529–541. [CrossRef] [PubMed]
16. Meinhold, J.; Arnold, E.; Isaacs, S. Effect of nitrite on anoxic phosphate uptake in biological phosphorus removal activated sludge. *Water Res.* **1999**, *33*, 1871–1883. [CrossRef]
17. Lee, H.; Yun, Z. Comparison of biochemical characteristics between PAO and DPAO sludges. *J. Environ. Sci.* **2014**, *26*, 1340–1347. [CrossRef]
18. Yun, G.; Lee, H.; Hong, Y.; Kim, S.; Daigger, G.T.; Yun, Z. The difference of morphological characteristics and population structure in PAO and DPAOgranular sludges. *J. Environ. Sci.* **2019**, *76*, 388–402. [CrossRef]
19. Guo, Y.; Chen, Y.; Webeck, E.; Li, Y.-Y. Towards more efficient nitrogen removal and phosphorus recovery from digestion effluent: Latest developments in the anammox-based process from the application perspective. *Bioresour. Technol.* **2020**, *299*, 122560. [CrossRef]
20. Xue, Y.; Ma, H.; Kong, Z.; Guo, Y.; Li, Y.-Y. Bulking and floatation of the anammox-HAP granule caused by low phosphate concentration in the anammox reactor of expanded granular sludge bed (EGSB). *Bioresour. Technol.* **2020**, *310*, 123421. [CrossRef]
21. Guo, Y.; Li, Y.-Y. Hydroxyapatite crystallization-based phosphorus recovery coupling with the nitrogen removal through partial nitritation/anammox in a single reactor. *Water Res.* **2020**, *187*, 116444. [CrossRef]
22. Xue, Y.; Ma, H.; Kong, Z.; Li, Y.-Y. Formation Mechanism of hydroxyapatite encapsulation in Anammox-HAP Coupled Granular Sludge. *Water Res.* **2021**, *193*, 116861. [CrossRef] [PubMed]
23. Kong, Y.H.; Liu, Y.Q.; Tay, J.H.; Wong, F.S.; Zhu, J.R. Aerobic granulation in sequencing batch reactors with different reactor height/diameter ratios. *Enzyme Microb. Technol.* **2009**, *45*, 379–383. [CrossRef]
24. Liu, Y.; Tay, J.H. The essential role of hydrodynamic shear force in the formation of biofilm and granular sludge. *Water Res.* **2002**, *36*, 1653–1665. [CrossRef] [PubMed]
25. Dulekgurgen, E.; Artan, N.; Orhon, D.; Wilderer, P.A. How does shear affect aggregation in granular sludge sequencing batch reactors? Relations between shear, hydrophobicity, and extracellular polymeric substances. *Water Sci. Technol.* **2008**, *58*, 267–276. [CrossRef] [PubMed]
26. Liu, Y.Q.; Tay, J.H. Influence of starvation time on formation and stability of aerobic granules in sequencing batch reactors. *Bioresour. Technol.* **2008**, *99*, 980–985. [CrossRef] [PubMed]
27. McSwain, B.S.; Irvine, R.L.; Hausner, M.; Wilderer, P.A. Composition and distribution of extracellular polymeric substances in aerobic flocs and granular sludge. *Appl. Environ. Microbiol.* **2005**, *71*, 1051–1057. [CrossRef] [PubMed]
28. Lopez-Vazquez, C.M.; Oehmen, A.; Hooijmans, C.M.; Brdjanovic, D.; Gijzen, H.J.; Yuan, Z.; van Loosdrecht, M.C. Modeling the PAO–GAO competition: Effects of carbon source, pH and temperature. *Water Res.* **2009**, *43*, 450–462. [CrossRef] [PubMed]
29. Oehmen, A.; Lopez-Vazquez, C.M.; Carvalho, G.; Reis, M.A.M.; Van Loosdrecht, M.C.M. Modelling the population dynamics and metabolic diversity of organisms relevant in anaerobic/anoxic/aerobic enhanced biological phosphorus removal processes. *Water Res.* **2010**, *44*, 4473–4486. [CrossRef]
30. Weng, C.N.; Molof, A.H. Nitrification in the biological fixed-film rotating disk system. *Water Pollut. Control. Fed.* **1974**, *46*, 1674–1685.
31. Frølund, B.; Palmgren, R.; Keiding, K.; Nielsen, P.H. Extraction of extracellular polymers from activated sludge using a cation exchange resin. *Water Res.* **1996**, *30*, 1749–1758. [CrossRef]
32. Lowry, O.H.; Rosebrough, N.J.; Farr, A.L.; Randall, R.J. Protein measurement with the Folin phenol reagent. *J. Biol. Chem.* **1951**, *193*, 265–275. [CrossRef] [PubMed]
33. Zhang, B.; Ji, M.; Qiu, Z.; Liu, H.; Wang, J.; Li, J. Microbial population dynamics during sludge granulation in an anaerobic–aerobic biological phosphorus removal system. *Bioresour. Technol.* **2011**, *102*, 2474–2480. [CrossRef] [PubMed]
34. de Kreuk, M.K.; van Loosdrecht, M.C. Formation of aerobic granules with domestic sewage. *J. Environ. Eng.* **2006**, *132*, 694–697. [CrossRef]
35. Saidou, H.; Korchef, A.; Ben Moussa, S.; Ben Amor, M. Struvite precipitation by the dissolved CO_2 degasification technique: Impact of the airflow rate and pH. *Chemosphere* **2009**, *74*, 338–343. [CrossRef] [PubMed]
36. Zhu, G.B.; Peng, Y.Z.; Wu, S.Y.; Wang, S.Y.; Xu, S.W. Simultaneous nitrification and denitrification in step feeding biological nitrogen removal process. *J. Environ. Sci.* **2007**, *19*, 1043–1048. [CrossRef] [PubMed]
37. Dsane, V.F.; Jeon, H.; Choi, Y.; Jeong, S.; Choi, Y. Characterization of magnetite assisted anammox granules based on in-depth analysis of extracellular polymeric substance (EPS). *Bioresour. Technol.* **2023**, *369*, 128372. [CrossRef] [PubMed]
38. Lv, L.; Feng, C.; Li, W.; Ren, Z.; Wang, P.; Liu, X.; Gao, W.; Sun, L.; Zhang, G. Accelerated performance recovery of anaerobic granular sludge after temperature shock: Rapid construction of protective barriers (EPS) to optimize microbial community composition base on quorum sensing. *J. Clean. Prod.* **2023**, *392*, 136243. [CrossRef]
39. Samaei, S.H.A.; Chen, J.; Xue, J. Current progress of continuous-flow aerobic granular sludge: A critical review. *Sci. Total Environ.* **2023**, *875*, 162633. [CrossRef]

40. Chuprunov, K.; Yudin, A.; Lysov, D.; Kolesnikov, E.; Kuznetsov, D.; Leybo, D.; Ilinykh, I.; Godymchuk, A. The pH level influence on hydroxyapatite phase composition synthesized with hydrothermal method. In *IOP Conference Series: Materials Science and Engineering, Proceedings of the International Science and Technology Conference for Youth "Advanced Materials for Engineering and Medicine", Tomsk, Russian, 30 September–5 October 2019*; IOP Publishing: Bristol, UK, 2020; Volume 731, p. 012023.
41. López-Ortiz, S.; Mendoza-Anaya, D.; Sánchez-Campos, D.; Fernandez-García, M.E.; Salinas-Rodríguez, E.; Reyes-Valderrama, M.I.; Rodríguez-Lugo, V. The pH effect on the growth of hexagonal and monoclinic hydroxyapatite synthesized by the hydrothermal method. *J. Nanomater.* **2020**, *2020*, 5912592. [CrossRef]
42. Jorand, F.; Boué-Bigne, F.; Block, J.C.; Urbain, V. Hydrophobic/hydrophilic properties of activated sludge exopolymeric substances. *Water Sci. Technol.* **1998**, *37*, 307–315. [CrossRef]
43. Li, X.M.; Liu, Q.Q.; Yang, Q.; Guo, L.; Zeng, G.M.; Hu, J.M.; Zheng, W. Enhanced aerobic sludge granulation in sequencing batch reactor by Mg^{2+} augmentation. *Bioresour. Technol.* **2009**, *100*, 64–67. [CrossRef] [PubMed]
44. Muda, K.; Aris, A.; Salim, M.R.; Ibrahim, Z.; van Loosdrecht, M.C.M.; Ahmad, A.; Nawahwi, M.Z. The effect of hydraulic retention time on granular sludge biomass in treating textile wastewater. *Water Res.* **2011**, *45*, 4711–4721. [CrossRef] [PubMed]
45. Owusu-Agyeman, I.; Eyice, Ö.; Cetecioglu, Z.; Plaza, E. The study of structure of anaerobic granules and methane producing pathways of pilot-scale UASB reactors treating municipal wastewater under sub-mesophilic conditions. *Bioresour. Technol.* **2019**, *290*, 121733. [CrossRef] [PubMed]
46. Kim, J.; Park, J.; Choi, H.; Lee, C. Performance and stability enhancement of methanogenic granular sludge process: Feed pre-acidification and magnetite-embedded granule formation. *Chem. Eng. J.* **2023**, *469*, 143864. [CrossRef]
47. Quoc, B.N.; Wei, S.; Armenta, M.; Bucher, R.; Sukapanpotharam, P.; Stahl, D.A.; Stensel, H.D.; Winkler, M.-K.H. Aerobic granular sludge: Impact of size distribution on nitrification capacity. *Water Res.* **2021**, *188*, 116445. [CrossRef]
48. van den Berg, L.; Pronk, M.; van Loosdrecht, M.C.; de Kreuk, M. Density measurements of aerobic granular sludge. *Environ. Technol.* **2023**, *44*, 1985–1995. [CrossRef]
49. Wang, D.; Fu, Q.; Xu, Q.; Liu, Y.; Ngo, H.H.; Yang, Q.; Zeng, G.; Li, X.; Ni, B.-J. Free nitrous acid-based nitrifying sludge treatment in a two-sludge system enhances nutrient removal from low carbon wastewater. *Bioresour. Technol.* **2017**, *244*, 920–928. [CrossRef]